

Switching-mode-dependent magnetic interlayer coupling strength in spin valves and magnetic tunnel junctions

Y. Pennec,¹ J. Camarero,² J. C. Toussaint,¹ S. Pizzini,¹ M. Bonfim,^{1,*} F. Petroff,³ W. Kuch,⁴ F. Offi,^{4,†} K. Fukumoto,⁴ F. Nguyen Van Dau,³ and J. Vogel¹

¹Laboratoire Louis Néel, CNRS, 25 avenue des Martyrs, B.P. 166, F-38042 Grenoble Cedex 9, France

²Departamento de Física de la Materia Condensada, Universidad Autónoma de Madrid, E-28049 Madrid, Spain

³Unité Mixte de Physique CNRS/Thales, Domaine de Corbeville, F-91404 Orsay, France
and Université Paris-Sud, F-91405 Orsay, France

⁴Max-Planck-Institut für Mikrostrukturphysik, Weinberg 2, D-06120 Halle, Germany

(Received 25 March 2004; published 18 May 2004)

We have studied the magnetization reversal dynamics of spin valves and magnetic tunnel junctions deposited on step bunched silicon substrates with a strong topological modulation. Our measurements show that the magnetization reversal is dominated by domain wall propagation at low field sweep rates and nucleation processes at high sweep rates. The magnetostatic orange peel coupling present in quasi-static conditions between the magnetic layers disappears when switching by nucleation becomes dominant. Micromagnetic simulations show that this phenomenon can be explained taking into account the modulated topology of the substrate.

DOI: 10.1103/PhysRevB.69.180402

PACS number(s): 71.45.Lr, 61.10.-i, 72.15.Nj

The recent interest in magnetic trilayers in which two ferromagnetic (FM) layers are separated by an ultrathin non-magnetic spacer layer is fueled by the occurrence of a variety of exciting effects like giant magnetoresistance,¹ tunnel magnetoresistance,² spin injection,³ or spin torque transfer,⁴ which are all highly interesting for applications and fundamental studies. The observation of these effects requires independent manipulation of the magnetization direction of the two magnetic layers, which interact by magnetic interlayer coupling. For thicknesses of the non-magnetic spacer layer above a few nanometers, the magnetic interlayer coupling is dominated by the so-called Néel “orange peel” coupling.⁵ This magnetostatic interaction appears when the topological profiles (or “roughnesses”) of the two interfaces of the spacer layer are correlated. The interaction between magnetic charges deposited at the sides of topological “bumps” at the two interfaces then favors the parallel alignment of the magnetization of the two FM films.⁵

The fast switching of the magnetization direction in magnetic trilayers like spin valves and magnetic tunnel junctions is an issue of increasing importance for applications. While several studies have focused on the static behavior of the orange peel coupling,^{6,7} there is a lack of experimental studies regarding its dynamic behavior, and it is usually assumed that the coupling is independent of the speed with which the magnetic field is applied. In this paper we show that, in the case of spin valves and magnetic tunnel junctions with a strong topological modulation, the Néel orange peel coupling can drastically reduce when the applied field sweep rate is increased. This reduction is caused by a change in the magnetization reversal mechanism, which is dominated by propagation of domain walls in the quasi-static regime and by nucleation of magnetic domains at high sweep rates. By extending Néel’s model⁵ to include the details of the sample topology and micromagnetic interactions on the nanometer scale, the strength of the observed coupling can be explained and the sweep-rate dependence of the magnetic coupling can be understood.

The trilayers studied in this paper were deposited on step bunched Si(111) substrates disoriented by 4° along the $[11\bar{2}]$ direction.⁸ A spin valve with layer structure Si/Cu(0.3)/Au(3)/Co(5)/Cu(10)/Fe₂₀Ni₈₀(5)/Cu(2)/Au(1.5) was prepared by molecular beam epitaxy.⁹ A magnetic tunnel junction with layer structure Si/Cu(0.3)/Co(15)/Al₂O₃(2)/Fe₂₀Ni₈₀(15)/Au(5) was deposited by rf sputtering.¹⁰ The numbers in brackets mean thickness in nm. The cross sectional transmission electron microscopy image of the tunnel junction in Fig. 1(a) shows that the topology of the Si substrate, consisting of large terraces separated by steps, is well transferred to the ferromagnetic layers. The atomic force microscopy image shown in Fig. 1(b) for the alumina barrier reveals a topological modulation along the $[11\bar{2}]$ direction of the substrate. Due to the nucleation mode of the step bunching mechanism,¹¹ terraces take the shape of elongated ellipses with a characteristic length of about $1\ \mu\text{m}$ and an average width of 63 nm. The height of the steps, which are present both in the x and the y directions [Fig. 1(b)], is about 6 nm.

Our previous studies of magnetization reversal using time-resolved x-ray magnetic circular dichroism (XMCD)¹² revealed that in these samples the magnetic coupling be-

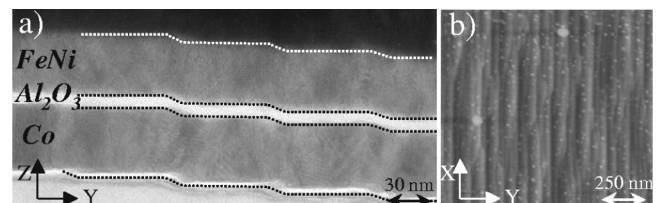


FIG. 1. (a) Cross sectional transmission electron microscopy image of the magnetic tunnel junction of structure Co(15 nm)/Al₂O₃(2 nm)/FeNi(15 nm). (b) Atomic force microscopy image of the tunnel junction taken after deposition of the alumina barrier.

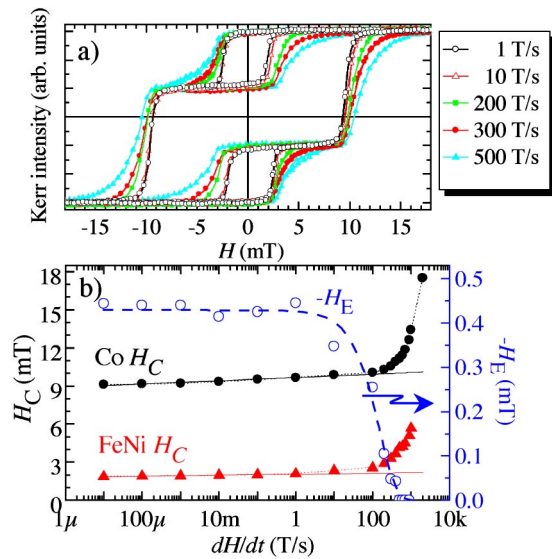


FIG. 2. (Color online) (a) Hysteresis loops of the Co(5 nm)/Cu(10 nm)/FeNi(5 nm) spin valve measured along the easy axis for several field sweep rates dH/dt . (b) dH/dt dependence of the coercivities H_C of the FeNi and Co films and of the interlayer magnetic coupling H_E obtained from the shift of the minor hysteresis loop of the FeNi layer. The lines are guides to the eye.

tween cobalt and permalloy layers observed in quasi-static conditions strongly decreases when magnetic pulses of some nanoseconds duration are applied. To determine the mechanism leading to this effect, we have measured by longitudinal Kerr effect the hysteresis curves of the spin valve and the tunnel junction using triangular shaped magnetic fields with sweep rates (dH/dt) ranging from quasi-static up to 2 kT/s. Due to the elongated shape of the terraces, both samples show a clear in-plane uniaxial anisotropy, with the easy magnetization axis parallel to the long axis of the terraces (x direction in Fig. 1(b)). The hysteresis curves measured with the field parallel to the easy magnetization axis show, for all dH/dt values, two transitions associated with the successive reversal of the permalloy (smaller coercivity) and the cobalt layer (larger coercivity). For low sweep rates the permalloy minor hysteresis loops are shifted with respect to zero field by about 0.4 mT. This shift is a measure of the magnetostatic coupling of the permalloy layer with the cobalt layer, induced by the layer topology. Some representative hysteresis loops of the spin valve sample are presented in Fig. 2(a). The FeNi and Co coercivities and the magnetic coupling between the two layers are reported in Fig. 2(b) as a function of dH/dt . Upon increasing the field sweep rate, the loops get less square and the coercive fields H_C increase. For low sweep rates, this increase of the coercivity is slow and logarithmic in dH/dt . For sweep rates around 100 T/s the increase of the coercivity with field sweep rate becomes much faster. This behavior has been explained in the literature in terms of a transition between two different reversal regimes.^{13,14} At low sweep rates the magnetization reverses mainly by domain wall propagation while at higher sweep rates successive nucleations of small reversed domains dominate the reversal.

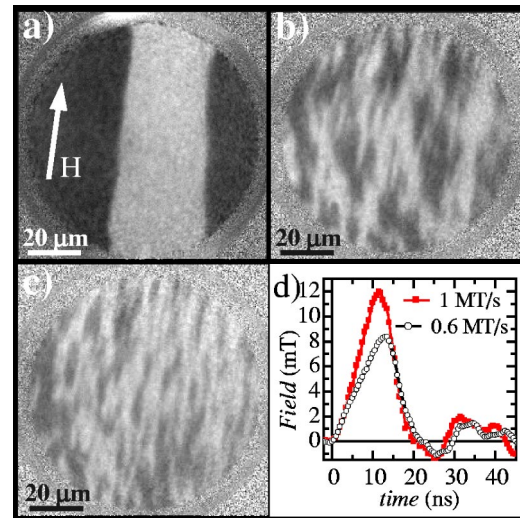


FIG. 3. (Color online) X-PEEM images showing the domain structure of the permalloy layer of the spin valve sample after application of magnetic pulses: (a) pulse 1 ms long and 2 mT high; (b) and (c) pulses 20 ns long with sweep rate values and amplitudes shown in panel (d). The pulsed field direction is indicated in (a) and is parallel to the easy magnetization axis.

The dynamic Kerr measurements reveal that the magnetic coupling between the two ferromagnetic layers, extracted from the shift of the permalloy minor hysteresis loop, drastically decreases at high sweep rates, starting from values corresponding to the transition between the two magnetization reversal regimes [Fig. 2(b)]. For dH/dt above 300 T/s the coupling vanishes. This is in agreement with our time-resolved XMCD data, which showed that for sweep rates around 10^6 T/s the two magnetic layers were virtually uncoupled.

To confirm experimentally the existence of two regimes for magnetization reversal at low and high sweep rates, we have performed x-ray photoelectron emission microscopy (X-PEEM) measurements of the spin valve sample. X-PEEM combines XMCD and PEEM to image the magnetic domain structure of thin films with element selectivity. Measurements were carried out at the UE56-2 helical undulator beamline in the synchrotron radiation source BESSY II (Berlin). The set-up of the microscope is described in Ref. 15. By tuning the x-ray photon energy to the Fe L_3 absorption edge, the domain structure of the permalloy layer was visualized. In Fig. 3(a) we show the domain structure obtained after saturation in the negative (dark) direction and application of a quasi-static 1 ms long and 2 mT high pulse in the opposite direction. One or two reversed domains have nucleated and subsequently their domain walls have propagated. If much shorter pulses with sweep rates of the order of 10^6 T/s are applied [Figs. 3(b) and (c)] the reversal mechanism changes drastically and a large number of small reversed domains is created. As dH/dt increases their density increases and their size decreases, indicating that at high sweep rates magnetization reversal by nucleation becomes more and more important. These observations were confirmed by recent time-resolved X-PEEM measurements on the spin-valve sample.¹⁶ These results strongly support the hypothesis that the disappearance of the orange peel coupling at high sweep rates is

associated with the transition to a magnetization reversal regime dominated by nucleation.

In order to explain the difference in magnetic coupling for the two reversal modes, the detailed topology of the samples has to be taken into account. We have first used the model proposed by Néel,⁵ corrected for the finite thickness of the magnetic layers,⁶ to calculate the static magnetic coupling between the two ferromagnetic layers separated by the non-magnetic spacer. In order to apply Néel's model to the step topology of our samples, we have used a Fourier series of sinusoidal roughness profiles. Since the magnetization is pointing along the long axis of the terraces, the coupling takes place only at the steps *perpendicular* to this axis, at both ends of the terraces. This model results in values for the coupling, localized at the steps, of $34.5 \mu\text{T}$ for the spin valve and $104 \mu\text{T}$ for the magnetic tunnel junction, but the average coupling integrated over the terrace area is practically zero. It should be noticed that since quasi-static reversal takes place through the nucleation of reversed domains and the subsequent propagation of domain walls [Fig. 3(a)], the coupling is not given by the mean value of the magnetostatic energy stored in one terrace, as in Néel's static model, but by the interaction of the domain wall with the steps localized at the end of the terraces. The coupling field calculated at these centers is however an order of magnitude smaller than the experimental value of 0.4 mT . A reason for this discrepancy could be that in Néel's model the coupling takes place between two relatively *flat* surfaces, with the roughness amplitude small with respect to the spacer thickness. In our case the height of the steps is of the same order of magnitude as the spacer thickness.

To overcome the limitations of Néel's model, we have performed two-dimensional micromagnetic simulations to describe the quasi-static FeNi magnetization reversal in terms of the interaction between a domain wall propagating in the permalloy layer and the magnetostatic charges deposited on the steps at the FeNi/Cu and Co/Cu interfaces. The numerical approach is based on the solution of the Landau-Lifschitz-Gilbert micromagnetic equation, which involves Zeeman energy and exchange and dipolar interactions.¹⁷ The only anisotropy term considered in the model is the one induced by the shape of the terraces.

In the case of our strongly modulated anisotropic system, we have to differentiate between the propagation of a domain wall in the direction perpendicular or parallel to the easy magnetization axis (respectively, the y and x directions in Fig. 1). We first consider a FeNi domain wall propagating along the hard axis direction, which needs to cross a step parallel to the long axis of the terraces. Since such a step is parallel to the Co magnetization direction, no magnetic charges are deposited on it and no magnetic coupling is induced between the two layers. We can then neglect the presence of the underlying Co layer and only consider the FeNi layer. When the Néel-type domain wall is located at the step, the magnetization at its center points in the direction perpendicular to the step and creates magnetic charges on it. In order to propagate, the domain wall has to cross an energy barrier associated to the demagnetizing field created by these charges. A value of 3.5 mT is found for FeNi thicknesses of

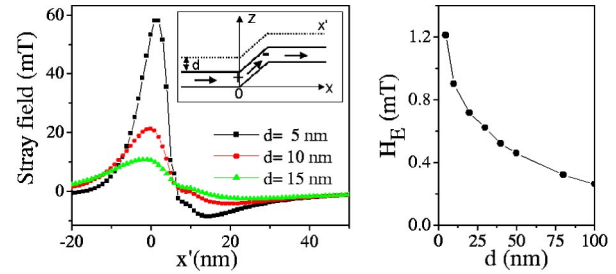


FIG. 4. (Color online) (a) x -component of the stray field emitted by a 5 nm thick Co film around a 6 nm wide topological step, calculated for a constant height of flight of 5 nm (squares), 10 nm (circles) and 15 nm (up triangles) from the Co surface. Inset: sketch of the profile of the Co layer and its magnetization (arrows) around a topological step perpendicular to the easy magnetization axis. The dashed line shows a typical constant height of flight line. (b) Calculated coupling field between FeNi and Co layers for different spacer thicknesses. The line is a guide to the eye.

5 nm . This “demagnetizing step” acts as a pinning center, tending to isolate the terraces one from another. This could explain why reversal following the Stoner-Wolffarth model¹⁸ has been observed in other samples deposited on step bunched substrates.¹⁰ If domain wall propagation is inhibited, the terraces can act as independent particles which satisfy the Stoner-Wolffarth model criteria, since they show uniaxial anisotropy and lateral dimensions below the domain wall width.

We now consider the propagation of a FeNi domain wall in the easy axis direction (x axis) over a step parallel to the hard magnetization axis. In this case, the magnetization direction at the center of the domain wall is parallel to the step and therefore does not charge it. The step acts as a pinning center for the propagation of the domain wall, because of the local magnetic coupling with the underlying Co layer (we call this a “coupling step”). Our simulations show that the magnetization direction in the Co layer follows the topological profile leading to the deposition of magnetic charges in the Co layer in the region of the steps. Figure 4(a) shows the calculated stray field generated by these charges. Its distribution is asymmetric with respect to the center of the step, and its maximum intensity can reach several tens of mT at 5 nm distance from the Co surface. The coupling field between FeNi and Co is then calculated as the difference in energy barrier for the propagation across the step of a 100 nm wide domain wall in FeNi in the directions parallel and anti-parallel to the Co magnetization direction. The values of the coupling field as a function of the distance between the two layers are shown in Fig. 4(b). For 10 nm distance the value of the coupling field is about 0.8 mT , in much better agreement with the experimental value of 0.4 mT than the one obtained with Néel's model.

Combining the experimental results and the simulations, we can now explain the disappearance of the magnetostatic coupling for high field sweep rates. At low speed, the FeNi reversal is dominated by domain wall propagation and the stray field associated with local charges deposited in the Co layer at the steps is responsible for the magnetic coupling. At high sweep rates, magnetization reversal is dominated by

nucleation. The reversed domains appear inside the terraces where the coupling is practically zero. No propagation of a domain wall over the steps is necessary to reverse the magnetization and the coupling becomes ineffective.

In conclusion, we have shown that to explain the magnetic properties of coupled magnetic layers with strong topological modulations, demagnetizing field effects at nanometric scales have to be taken into account. In order to understand the dynamic behavior of the magnetization reversal of Co/spacer/FeNi trilayers deposited on step bunched Si substrates, the static interpretation of the magnetostatic orange peel coupling has to be modified. The coupling is highly localized and caused by the interaction between the FeNi domain wall and the stray field of the Co layer around the steps. We have shown that the difference in reversal mechanism dominating quasi-static and dynamic reversal

can cause a drastic decrease of the “orange peel” coupling when the field sweep rate is increased. This decrease takes place when the switching mode changes from domain wall propagation to nucleation, since the local character of the interaction does not affect nucleation events. For coupled systems with a smoother morphology the difference between quasi-static and dynamic coupling will be less pronounced. However, given the different time and length scales that are implied, the use of parameters obtained from quasi-static measurements to explain dynamic reversal should be taken with care.

We are grateful to J. Humbert and A. Vaurès for their help and expertise in sample preparation. Thanks to J.-L. Maurice for the TEM experiments. J.C. acknowledges the support of the European Union through Contract No. HPMF-CT-1999-00151.

*Present address: Departamento de Engenharia Elétrica, Universidade do Paraná, CEP 81531-990, Curitiba, Brazil.

†Present address: INFM, Unità Roma Tre, Via della Vasca Navale 84 I-00146 Roma, Italy.

¹M.N. Baibich, J.M. Broto, A. Fert, F. Nguyen Van Dau, F. Petroff, P. Etienne, G. Creuzet, A. Friederich, and J. Chazelas, *Phys. Rev. Lett.* **61**, 2472 (1988); G. Binasch, P. Grünberg, F. Saurenbach, and W. Zinn, *Phys. Rev. B* **39**, 4828 (1989).

²J.S. Moodera, L.R. Kinder, T.M. Wong, and R. Meservey, *Phys. Rev. Lett.* **74**, 3273 (1995).

³Y. Ohno, D.K. Young, B. Beschoten, F. Matsukura, H. Ohno, and D.D. Awschalom, *Nature (London)* **402**, 790 (1999); A.T. Hanbicki, B.T. Jonker, G. Itskos, G. Kiioseoglou, and A. Petrou, *Appl. Phys. Lett.* **80**, 1240 (2002).

⁴E.B. Myers, D.C. Ralph, J.A. Katine, R.N. Louie, and R.A. Buhrman, *Science* **285**, 867 (1999); W. Weber, S. Riesen, and H.C. Siegmann, *ibid.* **291**, 1015 (2001).

⁵L. Néel, *C. R. Hebd. Seances Acad. Sci.* **255**, 1676 (1962).

⁶J.C.S. Kools, W. Kula, D. Mauri, and T. Lin, *J. Appl. Phys.* **85**, 4466 (1999).

⁷B.D. Schrag, A. Anguelouch, S. Ingvarsson, G. Xiao, Y. Lu, P.L. Trouilloud, A. Gupta, R.A. Wanner, W.J. Gallagher, P.M. Rice, and S.S.P. Parkin, *Appl. Phys. Lett.* **77**, 2373 (2000).

⁸M. Sussiaiu, F. Nguyen Van Dau, P. Galtier, A. Encinas, and A. Schuhl, *J. Magn. Magn. Mater.* **165**, 1 (1996).

⁹A. Encinas, F. Nguyen Van Dau, A. Schuhl, F. Montaigne, M. Sussiaiu, and P. Galtier, *J. Magn. Magn. Mater.* **198-199**, 15 (1999).

¹⁰F. Montaigne, P. Gogol, J. Briatico, J.L. Maurice, F. Nguyen Van Dau, F. Petroff, A. Fert, and A. Schuhl, *Appl. Phys. Lett.* **76**, 3286 (2000).

¹¹E.D. Williams and N.C. Bartelt, *Science* **251**, 393 (1991).

¹²M. Bonfim, G. Ghiringhelli, F. Montaigne, S. Pizzini, N.B. Brookes, F. Petroff, J. Vogel, J. Camarero, and A. Fontaine, *Phys. Rev. Lett.* **86**, 3646 (2001).

¹³E.M. Gyorgy, *J. Appl. Phys.* **28**, 1011 (1957).

¹⁴J. Camarero, Y. Pennec, J. Vogel, M. Bonfim, S. Pizzini, M. Cartier, F. Ernult, F. Fettar, and B. Dieny, *Phys. Rev. B* **64**, 172402 (2001).

¹⁵W. Kuch, R. Frömter, J. Gilles, D. Hartmann, Ch. Ziethen, C.M. Schneider, G. Schönhense, W. Swiech, and J. Kirschner, *Surf. Rev. Lett.* **5**, 1241 (1998).

¹⁶J. Vogel, W. Kuch, M. Bonfim, J. Camarero, Y. Pennec, F. Offi, K. Fukumoto, J. Kirschner, A. Fontaine, and S. Pizzini, *Appl. Phys. Lett.* **82**, 2299 (2003).

¹⁷J.C. Toussaint, A. Marty, N. Vukadinovic, J. Ben Youssef, and M. Labrune, *Comput. Mater. Sci.* **24**, 175 (2002).

¹⁸E.C. Stoner and E.P. Wohlfarth, *Philos. Trans. R. Soc. London, Ser. A* **240**, 599 (1948).